1620 Geographos and 433 Eros: Shaped by Planetary Tides

by

William F. Bottke, Jr.
Center for Radiophysics and Space Research
Cornell University
Ithaca, NY 14853-6801
bottke@astrosun.tn.cornell.edu
Tel: (607) 255-3934
Fax: (607) 255-9002

Derek C. Richardson,
Department of Astronomy
University of Washington
Box 351580
Seattle, WA 98185
(lcr{lastlc). }rasllillg(c)ll. cell]

Patrick Michel
Observatoire de Nice
B.P. 4229
06304 Nice Cedex 4
France
michel@rameau.obs-nice.fr

and

Stanley G. Love
Jet Propulsion Laboratory
M/S 306-438
4800 Oak Grove Drive
Pasadena, CA 91109-8099"
Stanley.G.Love@jpl.nasa.gov

Submitted to *Nature*
November 7, 1997

Main Text

Until recently, most asteroids were thought to be solid bodies whose shapes were determined largely by collisions with other asteroids [1]. It now seems that many asteroids are little more t hau rubble piles, held together by self-gravity [2]; this means that their shapes may be strongly affected by tides during close encounters with planets. Here we report numerical simulations of encounters between a rubble-pile asteroid and the Earth. After the encounter, many of the simulated asteroids have the same distinctive shape (i.e., highly elongated with a single convex side, tapered ends, and small protuberances swept back against the rotation direction) and rotation rate as 1620 Geographos. Our simulations indicate that asteroids affected by titles may often have small satellite companions, which were torn from the original body. We suggest that 433 Eros, which will be visited by the NEAR spacecraft in 1999, has been molded by tides and may therefore have a satellite.

The shapes of several Earth-crossing asteroids (ECAs) have now been inferred by delay-Doppler radar techniques [3]. The silhouette of the S-class asteroid 1620 Geographos (Fig. 1) has dimensions of 5.11 x 1.85 km (2.76 x 1.0, normalized), making it the most elongated object yet found in the solar system [4] [5]. Its rotation period (5.22 h) is short enough that loose mat erial is scarcely bound centrifugally near t he ends of t he body [6].

It has been suggested that Geographos's shape is diagnostic of a weak "rubble-pile" ast eroid distort ed 1 y t ides during a close planet ary encounter [7]. Several lines of evidence support t he idea that asteroids are oft en rubble piles, aggregates of smaller fragments held together by self-gravity rather than material strength: comet Shoemaker-Levy-9 (SL9) was tidally disrupted near Jupiter [8]; C-class asteroid 253 Mathilde has a remarkably low density (1.3 g cm^{-3}) [9]; of 107 asteroids smaller than 10 km, none has a rot at ion period shorter than 2.27 h, suggesting no strength [10]; numerical hydrocode simulations, used to model large crat er-forming events on Phobos, Gaspra, and Ida, suggest that rubble piles survive

better than coherent rock [11] [12] [13]. If the above data have been properly interpreted most km-sized ECAs are rubble piles [13], and thus, are susceptible to tidal distortion.

To assess the frequency at which Geographos has tidally important slow and close encounters with Earth (and Venus), we numerically integrated its orbit (a = 1.246 AU, e = 0.335, i = 13.34°) forward 4 Myr following the procedure of [14]. In view of the chaotic nature of orbits of ECAs [15] [16], we also integrated seven clones. In general, we determined their orbital evolution to be controlled by two mechanisms: close encounters with Earth and overlapping secular resonances ν_{13} and ν_{14} involving the mean precession frequencies of the nodal longitudes of Earth and Mars's orbits [15] [17]. We found that 5 of the 8 clones (62.5%) had their inclinations increased by these resonances, implying that these values were lower in the past. Similarly, 6 of the 8 clones (75%) had their orbital eccentricities increased by the ν_2 and ν_5 secular resonances with Venus and Jupiter. Lower eccentricities and inclinations in the past imply that close approaches near Earth were even more likely to occur, and to happen at the low velocities conducive for tidal disruption.

To investigate the effects of planetary tides on ECAs (cf. [7]), we used a sophisticated N-body code to model flybys between agglomerates of between 247 and 500 equal-sized spherical particles and the Earth [18] [19]. These numbers were chosen as a compromise between resolution and computational expediency [20] [21] [22]. For the same initial conditions, our N-body code reproduces the SL9 benchmark runs generated by other well-tested codes [8] [23]. We introduce, however, several improvements which allow more realistic simulations of tidal disruption: (a) we use progenitors with shapes similar to many ECAs (dimensions of 2.8 x 1.7 x 1.5 km) rather than spherical progenitors which are more stable against tidal disruption; (b) our model rubble piles rotate over a range of spin periods (P = 4, 6, 8, 10, 12, 20, and $P = \infty$ h) and spin axis orientations; most previous models ignored spin, which significantly aids tidal break-up; (c) our planetocentric trajectories are hyperbolic rather than parabolic; and (d) we incorporate friction and energy dissipation when particles collide; previous models often assured elastic or perfectly inelastic collisions.

The tidal effects experienced during an asteroid's close approach to Earth are deter-

mined by the asteroid's trajectory, rotation, and physical properties. We have systematically mapped these outcomes according to the asteroid's perigee distance q, approach speed v_∞, rotation period P, spin axis orientation, and orientation of the asteroid's long axis at perigee [18] [19]. Several distinct outcomes for tidal disruption are found, though here we concentrate on those that produce Geographos-type objects (i. e., a subset of those where up to 50% of object's initial mass is stripped off: objects losing more than 50% undergo Shoemaker-Levy-9-type disruptions).

Fig. 2 shows a "typical" outcome. The asteroid's equipotential surface to which a liquid would adapt is determined by incorporating local gravity, tidal and centrifugal terms. Near perigee, this surface becomes a more elongated ellipsoid with its longest axis oriented towards Earth. With a rubble pile, particles above the new angle of repose can roll or slide downslope to fill the "low spots", and thereby further modify the body's potential. As a consequence, the rubble-pile is elongated and, as the planet pulls on the body, its rotation rate altered. These forces can also bend one side of the body like bow, producing a convex shape on one size and a "hump"-like mound of material on the other.

Mass movement occurs when the total force on a particle near the asteroid's tips is insufficient to provide the centrifugal acceleration needed to maintain rigid body rotation. As clumps of material are lifted off the tips, they are swept backward in the equatorial plane by the asteroid's rotation. Material left behind frequently preserves this spiral signature as cusps pointing away from the rotation direction. In many cases, these fragments remain bound but separate from the model asteroid, creating a multiple system (a'hit]) sometimes dynamically evolves into a binary system. In simulations of tidal encounters, binaries make up $\sim 10\%$ of the entire km-sized ECA population, possibly explaining the observed population of doublet craters on the terrestrial planets [24] [25].

Topography also plays a role in the effectiveness of tidal deformation. The strength of tidal and centrifugal terms depends on each particle's position [26], such that some particles lie further above the local angle of repose than others. Since our model asteroid, like real ECAs, is neither a perfect ellipsoid nor a fluid, the new distorted shape is influenced by the

body's granular nature (i.e., friction and component size affect the strength of the landslide). Hence, particles leak more readily off one end than the other, often accentuated by limited particle movement before the rubble-pile reaches perigee. The ('11(1 that shed more mass frequently becomes elongated, tapered, and narrow when compared to the stubbier antipode. In addition, tidal forces stretch one side like a bow, giving the final product a shape much like ii "porpoise" or a "schmoo".

These characteristics, virtually identical to those seen on Geographos, are consequences of moderate-to-mild tidal disruptions. Roughly 15% of these events (scald from a set of 117 runs found over various values of q, v_∞, and P) stretch the Ills.jm axes to 2.5 or so times the size of the smaller axes. In addition, the median spin period for these distorted rubble piles is 5.2 h, the same as Geographos (5.221)).

Combining this dataset with estimates of ECA encounter probabilities and velocities with Earth and Venus [27], we find that a typical ECA should undergo all types of mass shedding once every ~ 65 Myr and a *moderate-to-mild* disruption event once every ~ 80 Myr (e. g., [19]), the former comparable to its collision rate with Earth and Venus. The most likely disruption candidates have low e's and i's, consistent with Geographos's probable orbital history. Since the dynamical lifetime of ECAs against planetary collision, comminution, or ejection by Jupiter is thought to be on the order of 10 Myr [28], we predict that $\sim 13\%$ of all ECAs undergo *moderate-to-mild* tidal disruptions, and that 2% should have highly-elongated shapes like Geographos.

Our success in suggesting an explanation for Geographos has led us to consider the next most elongated asteroid. S-class asteroid 433 Eros, the target of the NEAR mission. Like Geographos, Eros has a short rotation period (5.27 hours) [31] and a highly elongated shape (36 x15x 13 km, or 2.77x 1.2x 1.0, normalized [29] [30]: other shape estimates yield comparable results [31]). Even more intriguing, however, is Eros's pole-on silhouette, which, after delay-Doppler radar modeling, looks like a kidney bean (Fig. 3) [30]. It is likely that Eros's arched back and tapered ends are analogous to similar features on Geographos, themselves produced by spiral deformations associated with tidal forces. Additional comparisons can

be made once high resolution images from NEAR are obtained in 1999. Moreover, studies of Eros's orbit suggest that it may have been on a low-inclination deeply-crossing Earth-crossing orbit in the past; secular resonances (ν_4 and ν_{16}) were probably responsible for placing Eros in its current solely Mars-crossing orbit [14] [15] [17]. Given these properties, and the fact that tidal effects are, in general, stronger for larger objects [26], we suggest that Eros is also a tidally distorted rubble-pile. If true, then there is also a reasonable possibility that Eros has a small satellite produced by tidal fission (e.g., Fig. 2) [24].

Acknowledgments

We thank L. Benner, J. A. Burns, P. Farinella, S. Hudson, and S. Ostro for useful discussions.

References

[1] Davis, D. R., Weidenschilling, S. J., Farinella, P., Paolicchi, & Binzel, R. P. Asteroid collisional history: Effects on sizes and spins. In *Asteroids II* (eds. Binzel, R. P., Gehrels, T., & Matthews, M. S.), 805 826 (Univ. Arizona Press, Tucson, 1989).

[2] Burns, J. A. Small solar system bodies: The big picture. *ACM96* (in the press).

[3] Ostro, S. J. Planetary radar astronomy. *Rev.* Mod. *Phys.* **65**, 1235-1279 (1993).

[4] Ostro, S. J., et al. Extreme elongation of asteroid 1620 Geographos from radar images. *Nature* 375, 47-1-477 (1995).

[5] Ostro, S. J., et al. Radar observations of asteroid 1620 Geographos. *Icarus* 121, 46 66 (1996).

[(i] Burns, J. A. The angular momentum of solar system bodies: Implications for asteroid strengths. *Icarus* 25, 545 554. (1975).

[i'] Solem, J. C, & Hills, J. G. Shaping of Earth-crossing asteroids by tidal forces. *Astron. J.* 111, 13821387 (1996).

[8] Asphaug, E., & Benz, W. Size, density, and structure of comet Shoemaker-Levy-9 inferred from the physics of tidal breakup. *Icarus* 121, 225 248 (1 996).

[9] Yeomans, D. W., et al. The NEAR spacecraft's flyby of asteroid 253 Mathilde. *Science* (in the press).

[10] Harris, A. W. The rotation rates of very small asteroids: Evidence for "rubble-pile" structure. *Lunar Planet. Sci.* **XXVII**, 493494 (1996).

[11] Asphaug, E., & Melosh, H. J. The Stickney impact of Phobos A dynamic model. *Icarus* 101, 14-1164(1993).

[12] Greenberg, R., *et al.* Collisional and dynamical history of Ida. *Icarus* 120, 106–118 (1996).

[13] Love, S. G., & Ahrens, T. J. Catastrophic impacts on gravity dominated asteroids. *Icarus* **124**, 141–155 (1996).

[14] Michel, P., Froeschlé, Ch., & Farinella, P. Dynamical evolution of two near-Earth asteroids to be explored by spacecraft: 433 Eros and 4660 Nereus. *Astr. Astrophys.* 313, 993–1001" (1996).

[15] Michel, P., & Froeschlé, Ch. The location of linear secular resonances for semimajor axes smaller than 2 AU. *Icarus* 128, 230–240 (1997).

[16] Michel, P., Froeschlé, Ch., & Farinella, P. Dynamical evolution of NEAs - Close encounters, secular perturbations, and resonances. *Earth, Moon, & Planets* 72, 151–164 (1997).

[17] Michel, P. Effects of linear secular resonances in the region of semimajor axes smaller than 2 AU. *Icarus* 129, 348–366 (1997).

[18] Bottke, W. F., Richardson, D. C., & Love, S. G. Can tidal disruption of asteroids make crater chains on the Earth and Moon? *Icarus* 126, 470–474 (1997).

[19] Bottke, W. F., Richardson, D. C., & Love, S. G. Production of Tunguska-sized bodies by Earth's tidal forces. *Planet. Space Sci.* (in the press).

[20] Richardson, D. C. A new tree-code method for simulations of planetesimal dynamics. *Mon. Not. R. Astron. Soc.* 261, 396–414 (1993).

[21] Richardson, D. C. Tree-code simulations of planetary rings. *Mon. Not. R. Astron. Soc.* 269, 493–511 (1994).

[22] Richardson, D. C. A self-consistent numerical treatment of fractal ++qr('gate dynamics. *Icarus* **115**, 320–335 (1995).

[23] Boss, A. P. Cameron, A. G. W., & Benz, W. Tidal disruption of inviscid planetesimals. *Icarus* **92**, 165-178 (1991).

[24] Bottke, W. F., & Melosh, H. J. The formation of asteroid satellites and doublet craters by planetary tidal forces. *Nature* 381, 51-53 (1996).

[25] Bottke, W. F., & Melosh, H. J. The formation of binary asteroids and doublet craters. *Icarus* 124.372391 (1996).

[26] Hamilton, D. P., & Burns, J. A. Orbital stability zones around asteroids. *Icarus* 92, 118-131 (1996).

[27] Bottke, W. F., Nolan, M. C., Greenberg, R., & Kolvoord, R. A. Collisional lifetimes and impact statistics of near-Earth asteroids. In *Hazards Due to Comets and Asteroids* (eds. Gehrels, T., & Matthews, M. S.). 337-357 (Univ. Arizona Press, Tucson, 1994).

[28] Gladman, B. J., et al. Dynamical lifetimes of objects injected into asteroid belt resonances. *Science 277, 197-201* (1997).

[29] Zellner, B. Physical properties of asteroid 433 Eros. *Icarus* 28, 149-153 (1976).

[30] Mitchell, D. L., et al. Shape of asteroid 433 Eros from inversion of Goldstone radar Doppler spectra. *Icarus* (in the press).

[31] McFadden, L. A., Tholen, D. J., & Veeder, G. J. Physical properties of Aten, Apollo, and Amor asteroids. In *Asteroids II* (eds. Binzel, R. P., Gehrels, T., & Matthews, M. S.). 442-467 (Univ. Arizona Press, Tucson, 1989).

[32] http://echo.jpl.nasa.gov/asteroids/1620_Geographos/geographos.html.

Figure Captions

Figure 1: 1620 Geographos's pole-on silhouette determined from delay-Doppler observations taken in the asteroid's equatorial plane [4] [5]. This image has been constructed from multi-run sums of twelve co-registered images, each 30° wide in rotation phase space. The central white pixel indicates the body's center-of-mass. Rotation direction is indicated by the circular arrow. Brightness indicates the strength of radar return, arbitrarily scaled. Despite substantial smearing of the periphery features, some distinguishing characteristics can be observed: (i) The long axis is tapered on both ends, with one tip narrow and the other more pinched and squat. (ii) One side is smooth and convex; the opposite side has a "hump". (iii) Cusps at each end are swept back against the rotation direction, giving the body the appearance of a pinwheel when viewed from various aspect angles. The bottom figure shows four of the twelve summed co-registered 30° images used to make this silhouette. The resolution is 500 ns × 1.64 Hz (75 × 87 m). The cusps are more prominent here, though considerable smearing remains. For better resolution, a movie containing 150 delay-Doppler frames can be viewed at [32].

Figure 2: Four snapshots of the tidal breakup by the Earth of a 2 g cm^{-3} asteroid. Each of the 491 particles in the approaching ECA is 255 m in diameter and has a density of 3.6 g cm^{-3}, similar to ordinary chondritic meteorites. For this run the asteroid spin period starts at P = 6 hours prograde (i.e., when the dot product of the spin and orbital angular momentum vectors in planetocentric coordinates are positive), the perigee distance is $q = 2.1 R_{\oplus}$, and the encounter velocity at great distance is v_{∞} = 8 km s^{-1}. Fig. 2a shows the asteroid before encounter. The spin vector is normal to the orbital plane and points directly out of the page. Fig. 2b shows the body shortly after perigee passage. Differential forces, greatest at perigee, and centrifugal effects combine to set the particles into relative motion, producing a landslide towards the ends of the body. The action of the Earth stretches the model asteroid and, by pulling on the distorted mass, spins it up, increasing its total angular momentum. Shed mass

is frequently injected into orbit around the model asteroid, producing a binary. Fig. 2c shows the latter stages of the landslide. Particles near the tips drift backwards relative to the main body, forming cusps on each end. Note that these cusps are easy to create but difficult to retain with identical spherical particles at this resolution; we predict that real rubble piles, with rough or craggy components, would more readily "freeze" in position near the ends. Spiral distortion associated with tides produces a smooth convex surface along the long axis, and a "hump"-like mound of material on the opposing side. Fig. 2d shows the final shape of the object. The spin (P = 5.03 h) and elongation ($\sim$ 2.9 times the mean diameter of the minor axes) are virtually identical to Geographos (Fig. 1).

Figure 3: Pole-on silhouette of Eros, based on model where radar data were fit to a reference ellipsoid using 508 triangular facets defined by 256 vertices [30]. The silhouette is viewed from the asteroid's south pole at zero rotation phase with the radar at the bottom. Definitions for center of figure, center of rotation, and rotation direction are the same as given in Fig. 1. The body is tapered along its length, with a smooth convex side on the right side and one or more concavities on the left, making it look something like a kidney bean. Resolution does not permit interpretation of the concavities on the left side (i.e., whether they are craters, troughs, or bends in Eros's shape).

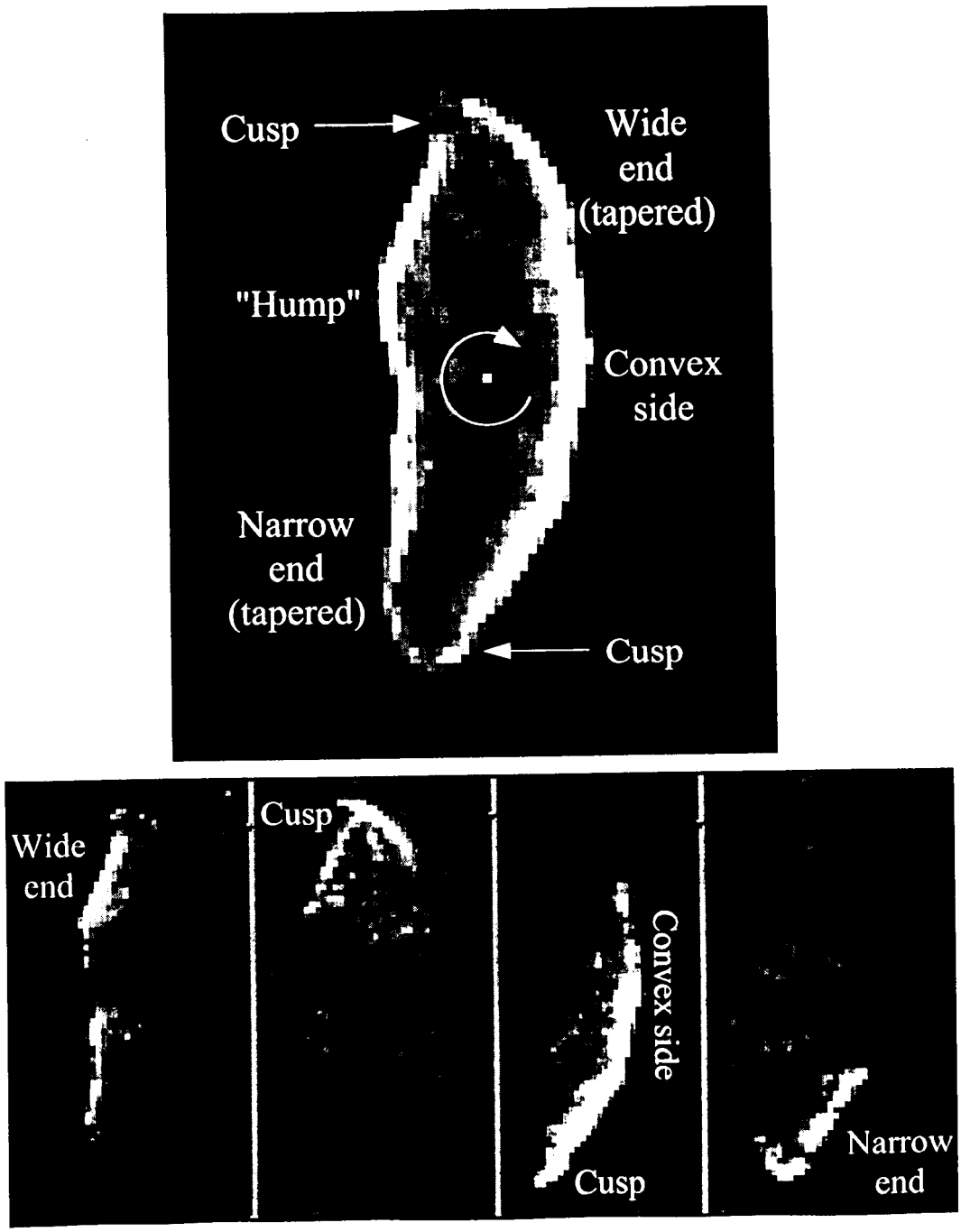
Cusp
Wide end (tapered)
"Hump"
Convex side
Narrow end (tapered)
Cusp
Wide end
Cusp
Convex side
Cusp
Narrow end

Figure 1: